
EXPERIMENTAL STUDY OF THE EFFECT OF THE ARM-LENGTH ON THE PERFORMANCE OF LOW-SPEED VERTICAL AXIS CURRENT TURBINEATEF SALEM M. SOUFALJEN^{1,*} ADI MAIMUN²¹Traning Department, Libyan Navy Forces, Tripoli, Libya²Marine Technology Centre, School of Mechanical Engineering

Universiti Teknologi Malaysia, Johor, MALAYSIA

atefsalem2000@gmail.com

ABSTRACT:

Additional alternative energy sources are needed to satisfy Libya's and other countries' rapid economic development and growing energy demand. Many governments, recognizing this necessity, passed the National Green Technology Policy few years ago to promote the use of green technology for activities that promote economic growth. Rivers, coastlines and ocean provide promising sources of renewable energy. The Low-Speed Vertical-Axis Current Turbine (LS-VACT) is a drag device that can be used to harness current energy from Mediterranean Sea, which tend to be characterised by low-speed currents. Unlike the Savonius rotor, the LS-VACT features arms attaching buckets to the main shaft. This increases the turbine's torque by increasing the leverage applied, thereby increasing the power generated. Additionally, the turbine is potentially suitable for deployment in remote areas. This paper presents an experimental investigation of the effect of arm lengths of 0.2, 0.27, and 0.34 metres on the performance and power take-off of the LS-VACT at a low-speed velocity of 0.32 m/s. The results indicate that changes in arm length have a significant effect on the performance of the turbine at the aforementioned speed. Peak power is achieved at an arm length of 0.27 metres, with $C_p=0.19$, $C_t=0.52$ and $\lambda=0.29$.

Keywords: Renewable energy, vertical axis current turbine, low speed, arm effect, power take-off, MAT LAB/Simulink

1. Introduction

At present, there is a strong interest in the development of renewable energy sources such as wind, ocean, and solar energy. Literature documents potential resources that can be harnessed for renewable energy in marine and coastal environments, including tidal motion, waves, currents, thermal gradients, and salinity gradients [1, 2]. If utilized, these marine renewable energy resources could potentially contribute to energy supply security and help reduce CO₂ emissions (as well as their impacts on the immediate surroundings and on the environment at large). Moreover, renewable energy generation efforts can improve the quality of life and create jobs in the local area (particularly in sectors tied to innovation).

The methods available to harness ocean energy resources include hydro turbines, which utilise marine current energy to generate power. These systems are divided into two types based on the kind of turbines they employ: either vertical-axis or horizontal-axis turbines. Both are effective power generation devices, per research literature [2-4]. Marine current turbines (MCT) and tidal current turbines (TCT) have competitive advantages over other renewable energy sources, including their predictability, their regularity, and their low environmental impact [5]. Thus, hydro turbines are considered to be among the most promising renewable energy conversion devices[6].

The sea surrounding Malaysia has the potential to provide a substantial amount of renewable energy from current, tidal and wave energy sources. Many studies have been carried out to demonstrate the feasibility of these power generation methods for Malaysia. The government's Economic Transformation Programme (ETP) initiative considers tapping the nation's hydroelectricity potential a key objective, defining hydroelectricity as one of the twelve National Key Economic Areas (NKEA) for Oil, Gas and Energy [7]. Because potential sites for hydroelectricity are mainly located in rural areas (such as near rivers and islands), hydroelectricity is also counted as one of the six National Key Result Areas (NKRA) for improving rural infrastructure [8].

At present in Malaysia, significant attention is being paid to the notion of using vertical-axis marine current turbines (drag device type) to extract energy from water flows with low stream velocity [9–12]. This type of MCT is omnidirectional (i.e., it can generate power from a current flow regardless of the device's orientation). It can accept the drag

force of the current flow with good starting characteristics, and it can operate at low current speeds.

Current speed and water depth are the most important factors in terms of MCT effectiveness [13]. Literature documents that a current speed of at least 2 m/s (4 knots) is ideal for turbine operation. However, as reported by the Royal Malaysian Navy [14], Malaysia's waters have an average current speed of only 0.56 m/s (1.1 knots). This velocity is only about half of the required minimum operational velocity for most turbines currently in use in other countries [13]. As a result, a larger turbine system than would normally be used is required to harness the current energy [13]. Because blade size is limited to water depth, however, certain shallow sites cannot accommodate larger turbines. Recently, researchers have proposed and tested a Savonius vertical-axis turbine to harness current energy from Malaysian waters, which tend to have low current speeds and shallow depths [12, 14]. This turbine was difficult to integrate with a generator due to the insufficient torque it generated. In addition, Libya has a sea with low-speed current, which is not suitable condition to extract the current energy. More specifically, the researchers suggest that 4 knots (2 m/s) is the minimum ideal marine current velocity for a turbine's operation. [13] Meanwhile, the Mediterranean Sea has an average current speed of only in the open sea is about 0.5 to 1 km/h (0.14 to 0.28 m/s), but in the straits, which act like a jet of wind, it can increase to 2 to 4 km/h (0.56 to 1.1 m/s). The Gulf Stream moves at 6 to 10 km/h (1.6 to 2.78 m/s). In other study, the maximum current velocities for the Mediterranean Sea were analysed and documented annually and seasonally from 2016 to 2018. [23] The highest recorded velocities reached 2.2 m/s in 2016 and 2017 and increased to 2.7 m/s in 2018. Seasonal assessments indicated the following maximum velocities for the years 2016 to 2018: 2.2 m/s for winter, 2.7 m/s for spring, 2.0 m/s for summer, and 2.1 m/s for autumn. [23]

The LS-VACT, with its novel features, appears to be more suited to harnessing marine energy from low-speed currents. The advantage of this marine turbine lies in its having four suitable blades attached to arms that maintain the device's high torque (even with the reduction of blades height). This allows the LS-VACT to rotate loaded turbines more efficiently.

A prototype turbine integrated with electrical interfaces (such as control, power stages, etc.) must be tested to validate the effectiveness of a novel turbine system.[15] There have been attempts to design a low-speed permanent magnet generator (PMG) for use as a direct drive generator to generate electricity from tidal currents with very low velocities [16, 17]. However, these generators require a high torque to operate the generator efficiently, as the principal goal of this design is to maximise a turbine's electric power output. Very few researchers have examined the effects of torque-augmenting arm constructions on the performance of current turbine models. Li and Calisal [18] reported that arms affect the power output of a turbine by producing extra drag and causing hydrodynamic interactions between the arms, shaft, and buckets or blades. Li and Calisal [18] studied the profile of the arm's cross section on modelling a vertical-axis tidal current turbine (Darrieus type) using a vortex method. They reported that the shape of the arms affects the turbine's performance due to the drag produced by the arms only. Moreover, Li and Calisal reported that heavier arms require special arm-blade connections, which increase the drag and can cause dynamic stall by increasing the inertia of the entire turbine system. In addition, Li and Calisal [18] found that the arm and shaft also have an effect on the turbine's noise intensity. In sum, the researchers reported that arms have effects on both the drag of the turbine and on its noise intensity. However, arms can also affect the turbine's performance/power output by decreasing/increasing the torque of the turbine.

For these reasons, this study employs an experimental approach to investigate the effect of the arms on the overall performance of the turbine. This study also provides a simulation model for predicting the electric power output of the turbine and demonstrating the effectiveness of a complete system.

2. Model

The turbine in this study is based on a full-scale prototype of a conventional Savonius turbine. The Savonius rotor has been proposed to be suitable for use in Malaysian waters with low-speed currents and low water depths [12, 14]. The main details of the full-scale prototype and the LS-VACT scaled (1:10) model, as well as the estimated dimensions of the LS-VACT, are presented in Table 1. The functional and dimensional principal sketches and the Schematic drawing of the LS-VACT are shown in Figures 1 and 2, respectively.

Table 1: The principal particular of the LS-VACT

No	Specification	Prototype LS-VACT			Model LS-VACT		
1	Height of Rotor, H(m)	14			1.4		
2	Diameter of the bucket, d (m)	2			0.2		
3	Scale factor	1:10					
4	Current Speed, U_{∞} (m/s)	0.5 & 1 & 2			0.17 & 0.32 & 0.64		
5	Blade Area, A_s (m ²)	28			2.8		
6	Diameter of Turbine, D_p (m)	8	9.4	10.8	0.8	0.94	1.08
7	Arm length, r' (m)	2	2.7	3.4	0.2	0.27	0.34
8	Arm length (lever), r (m)	3	3.7	4.4	0.3	0.37	0.44

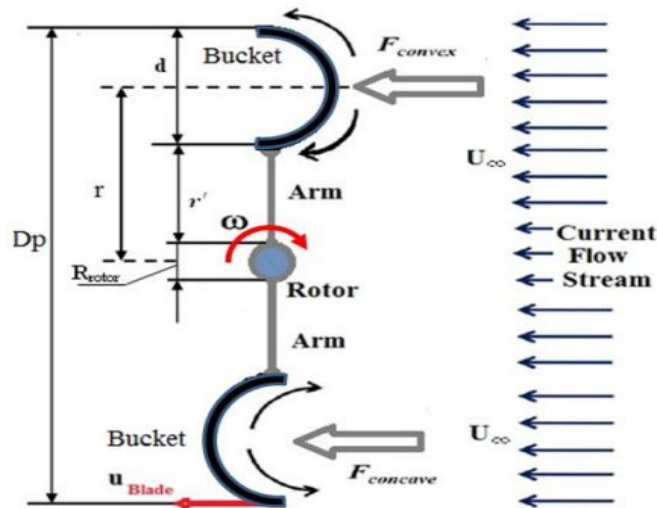


Fig. 1: A functional and dimensional principal sketch of the LS-VACT

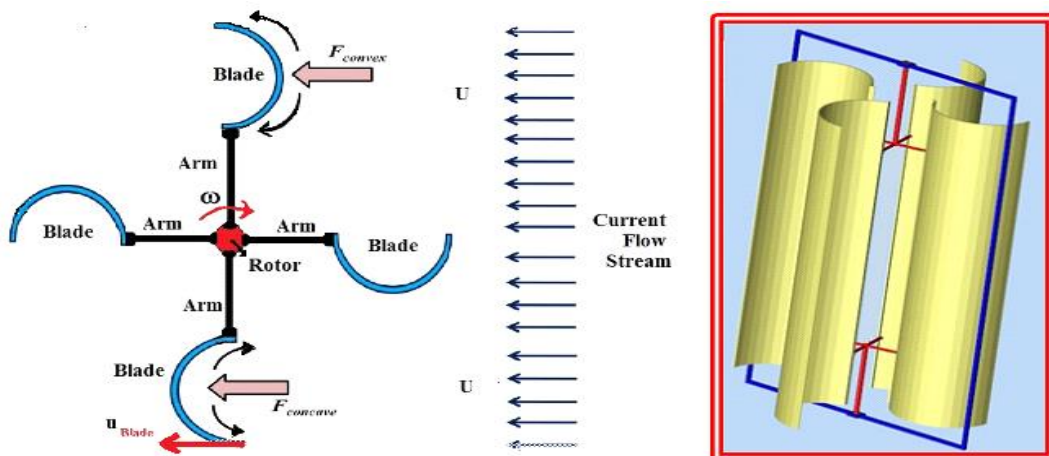


Fig. 2: Schematic drawing of the LS-VACT

3. Approach

This study involved conducting a series of experimental tests in order to determine the torque, angular velocity, and mechanical power of the turbine. Three different arm lengths were tested at an average current speed of 0.32 m/s to detect the effects of arm length on the turbine's performance. Measurements of rotational velocity, current speed, angular position, and turbine support torque were recorded simultaneously. The mechanical power for the LS-VACT was determined by measuring the mechanical torque on the rotating shaft and multiplying the rotational speed recorded at different arm lengths and current speeds [19]. The turbine with the best arm length performance was further subjected to current flow velocities of 0.17 m/s and 0.64 m/s. Next, the non-dimensional coefficients obtained from the experimental tests were incorporated into a computer simulation program to predict full-scale performance and power take-off. To simulate the forces produced at various current flow velocities, the buckets were subjected to drag tests at different azimuth angles of 0:30:180°. Both the concave and convex sides of the LS-VACT buckets were tested.

3.1 LS-VACT Experiment Setup and Test Procedures

Most past research has used a load mass technique to investigate turbine performance [19–22]. In these studies, the turbine is connected to a torque measurement arrangement using a load cell to capture the torque and a laser tachometer to measure the RPM. The arrangement used for the experimental setup is shown in Figures 3, 4 and 5. It contains a pulley system, special steel string, weighing pan, infrared optical tachometer, potentiometer and load cell. The weighing pan, pulley and load cell are connected by a string with a 1-mm diameter as shown in Figures 4 and 5. The tests had been performed in a towing tank operated by the Marine Technology Centre (MTC) at Universiti Teknologi Malaysia (UTM). This tank has a total length of 120 metres, a width of 4 metres, and a depth of 2.5 metres. The blockage coefficient, which is just 0.056, is small enough to be ignored (blockage was defined as the ratio of the water turbine's swept area with respect to the cross-sectional area of the submerged section of the towing tank). The LS-VACT was mounted to a specialized carriage and towed along the tank at constant velocities of 0.17, 0.32 and 0.64 m/s to simulate various flow stream speeds acting on the buckets of the LS-VACT. The RPM and force data were recorded and edited using a data acquisition system (DEWE 16) and personal computer (PC) as shown in Figure 3.

For this test, three ball bearings (SKF type) are mounted to the middle steel plates in order to support the LS-VACT rotor shaft. The weighing pan, pulley, and load cell are connected by a steel string of 1-mm diameter as shown in Figure 5. A process whereby the pulleys, the weighing pan, and the LS-VACT shaft were aligned was performed to ensure accurate measurements for all experiments. In order to reduce and minimize friction, which can affect measurements, the bearing's grease was removed and replaced with a standard oil solution. The surfaces of the grooves of the pulleys were also cleaned and smoothed to minimize skin friction drag. In addition, all sensors used in the study were calibrated prior to beginning to ensure consistent results.

The test began by running the LS-VACT without a load. After this, the LS-VACT was loaded gradually so that the load cell reading, weights, and rotational speeds of the rotor could be recorded. The mechanical power of the turbine was calculated using Equation (1). The load cell, a potentiometer, and an infrared optical tachometer were used to measure the associated torque and RPM.

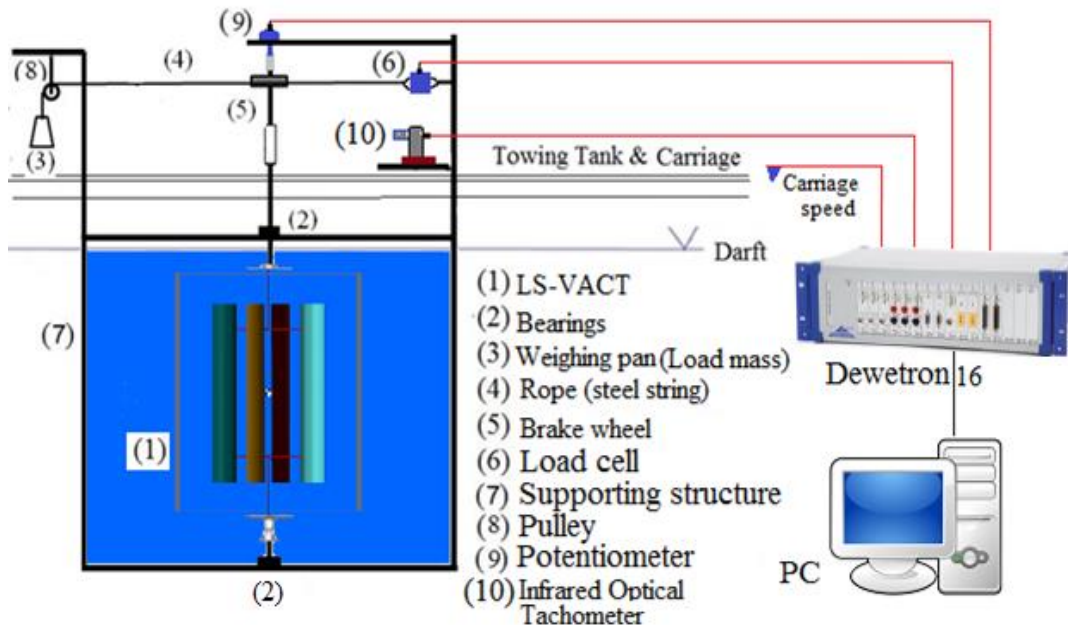


Fig. 3: The arrangement used for the experimental setup

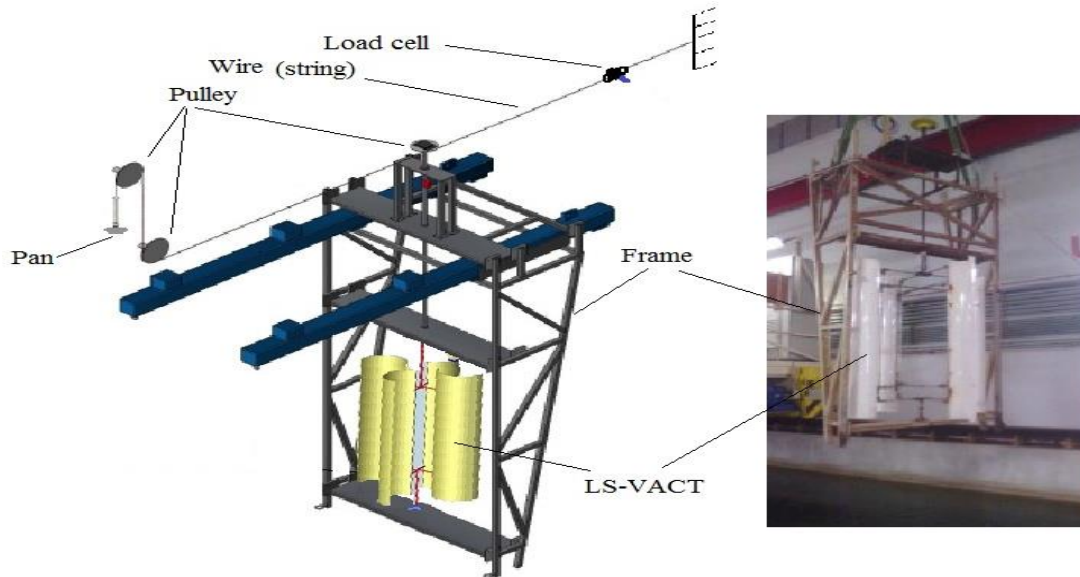


Fig. 4: The test rig of the LS-VACT

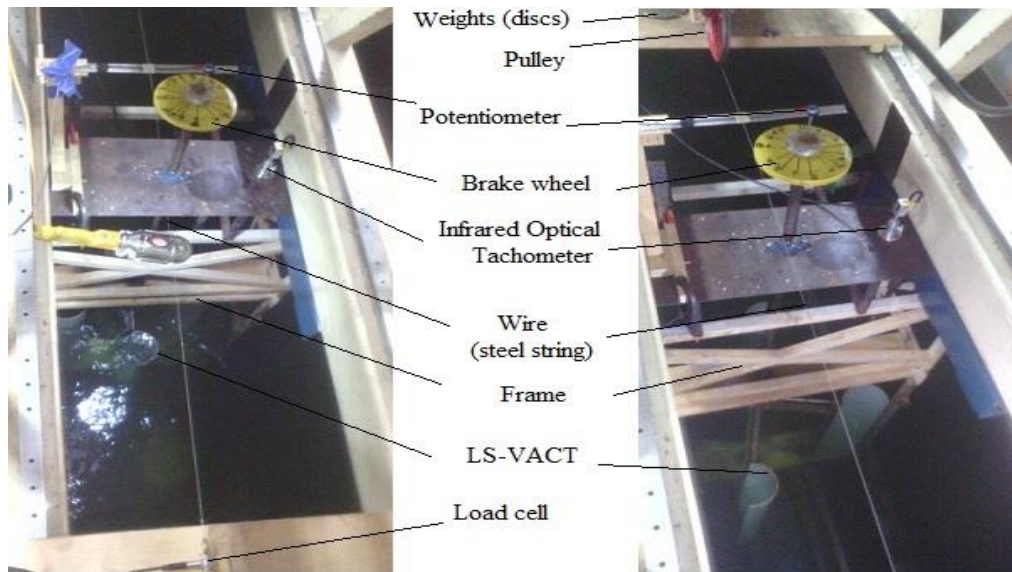


Fig. 5: The arrangement used for the experimental setup

In this experiment, various dead weights measuring between 0 and 20.2 kg (maximum load) were used to find the tangential force acting on the pulley. Dead weight was added gradually, and the corresponding rotational speed was recorded until the turbine stopped rotating, signalling that the flow stream current was no longer sufficient to turn it. The tangential force acting on the pulley was obtained by finding the difference between the tension forces imposed on the rope by dead weights and load cell recordings, as shown in Equation (4).

In order to ensure the replicability of the results and the precision of the measurements, the tests were repeated multiple times for each set of conditions. The repeated experiments showed close agreement between the results of successive trials. Based on the values measured for mechanical torque and angular velocity (derived from the rotational speed records), mechanical power can be estimated at each current speed as follows:

$$P_m = T \cdot \omega \quad (1)$$

Where 'T' is the mechanical torque and ' ω ' is the angular speed. The angular speed is defined in rad/s as:

$$\omega = 2 \cdot \pi \cdot n / 60 \quad (2)$$

Where 'n' is the shaft rotational speed in rpm, and the mechanical torque of the turbine is obtained in (N.m) by:

$$T = F \cdot r \quad (3)$$

Where: 'r' is the pulley radius plus the wire radius. Then, the force acting on the rotor can be obtained in (N) by:

$$F = (m - s) \cdot g \quad \rightarrow \quad F = m \cdot g - S_{lc} \quad (4)$$

Where 'm' is the mass loaded on the pan in kg, 's' is the spring balance reading in kg, ' S_{lc} ' is the load cell reading in N and 'g' is the gravitational acceleration. The power coefficient ' C_p ' and static torque coefficient ' C_{ts} ' can be determined from the following equations:

$$C_p = P_m / P_w \quad (5)$$

$$C_{ts} = \frac{4T}{\rho A D U_\infty^2} \quad (6)$$

Where ' P_w ' is calculated from the following equation:

$$P_w = 0.5 \cdot \rho \cdot A \cdot (U_\infty)^3 \quad (7)$$

Where ' ρ ' is water density, kg/m^3 , 'A' is the projected area of the turbine ($H \cdot d$), m^2 and ' U_∞ ' is the current speed, m/s. Finally, the power coefficient can be formulated as:

$$C_p = n \cdot r \cdot \pi \cdot (m \cdot g - S_{lc}) / 15 \cdot \rho \cdot A \cdot (U_\infty)^3 \quad (8)$$

3.2 One-Blade Straight Line Test (Turbine Bucket Oblique Test)

A bucket straight line test is conducted by attaching the turbine bucket to a 6-component force measuring system as shown in Figures 6 and 7. This system is mounted on the towing tank carriage. The model moves with towing carriage both in the towing direction and backwards. In the experiment, the bucket was towed along the tank at different carriage speeds to simulate the desired water flow velocities. Then, the forces acting on

the concave and convex surfaces of the bucket were measured using transducers. Forces were measured at 30° intervals relative to the bucket angle using the data acquisition system (DEWE 30 – 32). The speed and force data were recorded and edited. In addition, to ensure accurate results, the 6-component force system used in this test was calibrated prior to the trials. In order to confirm the results (and to ensure their replicability), the experiment was repeated several times under certain conditions. The results showed good agreement between successive measurements.

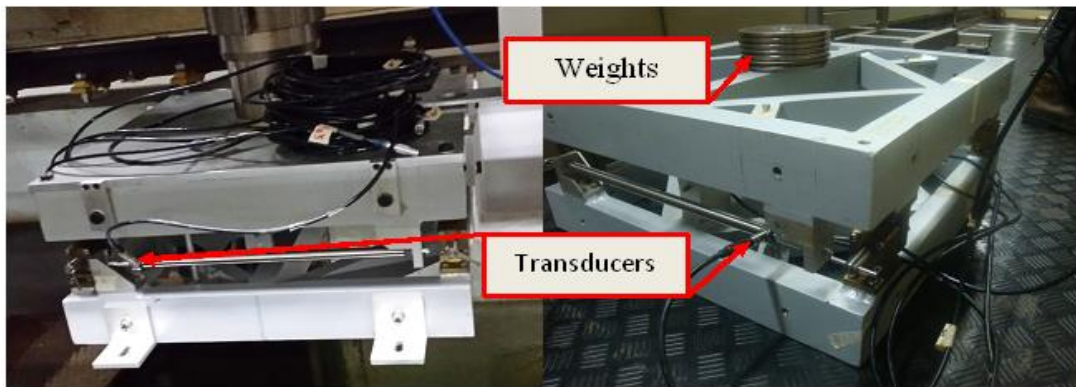


Fig. 6: The 6-component measurement system and its calibration process

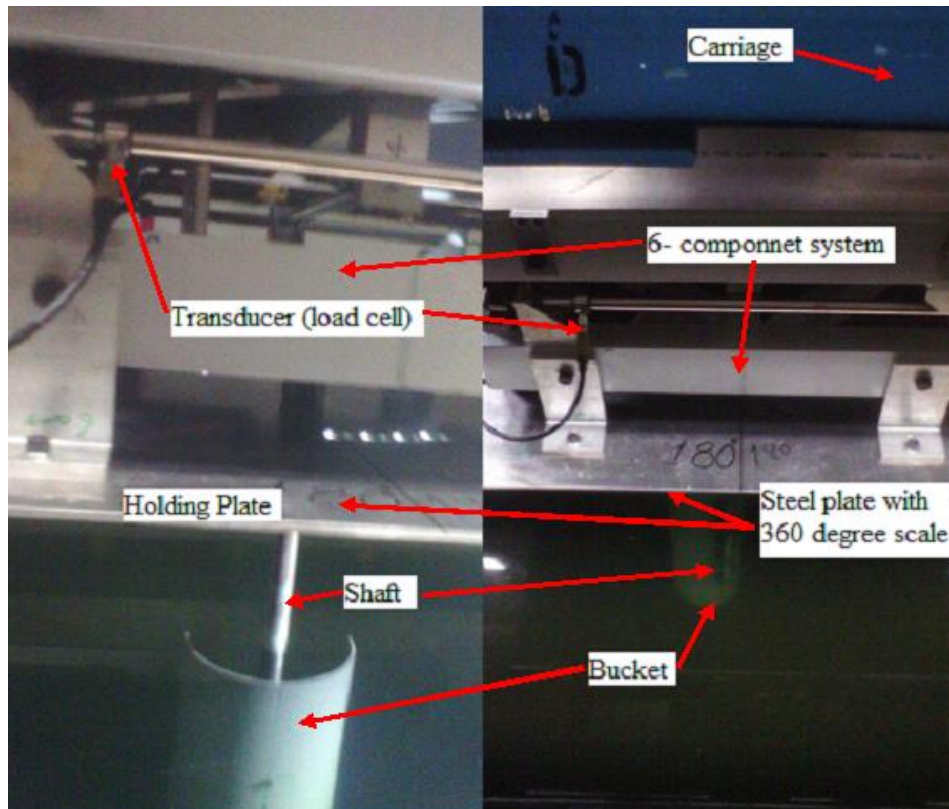


Fig. 7: The bucket is attached to the 6-component measurement system

Two components of drag force are generated on each blade surface. Normal drag force (F_d) acts perpendicular to the blade surface, and tangential drag force (F_T) acts on each bucket along a tangential direction. The drag coefficient was calculated using the set of equations in Equation (9).

$$\text{Drag Coefficient: } C_d = \frac{F_d}{0.5 \cdot \rho \cdot A \cdot U_\infty^2} \quad (9)$$

4. Results and Discussion

The experiments were carried out with for arm lengths of 0.2, 0.27 and 0.34 metres at a current speed of 0.32 m/s to determine the effects of arm length on the performance of the LS-VACT. The mechanical power and torque results are shown in Tables 2, 3, and 4. The maximum values for power and torque are illustrated in Figure 8. The results of the LS-VACT model tests indicate that the turbine with an arm length of 0.27 metres has a greater power output and higher maximum torque than turbines with arm lengths of 0.2 and 0.34 metres. An arm length of 0.27 metres was selected on the basis of the model tests, which showed the highest power output and torque magnitudes for that length. The results also showed that arm length has a different effect on power at a constant current speed (0.32 m/s). By changing the length of the arm (r') with respect to the blade chord (d) from a value of $r' = d$ to $r' = 1.35d$, the mechanical power of the LS-VACT increased by about 48%. The torque increased by 91% as well.

Table 2: Test results of the performance of the LS-VACT with arm length =0.2 m

No	Load (kg)	U_∞ (m/s)	RPM	Angular velocity (Rad)	TSR (λ)	Torque (N.m)	Mechanical Power (W)
1	0	0.32	5.86	0.61	0.78	-	-
2	1.15	0.32	4.38	0.46	0.58	0.77	0.35
3	2.15	0.32	4.50	0.47	0.59	1.42	0.66
4	3.15	0.32	4.13	0.43	0.55	2.03	0.88
5	4.15	0.32	3.70	0.39	0.49	2.65	1.03
6	5.15	0.32	3.33	0.36	0.45	3.25	1.17
7	6.15	0.32	2.81	0.29	0.37	3.85	1.13
8	7.15	0.32	2.52	0.2644	0.33	4.38	1.16
9	8.15	0.32	1.9	0.199	0.25	5.02	1.00
10	8.5	0.32	0	0	0	5.33	0

Table 3: Test results of the performance of the LS-VACT with arm length =0.27 m

No	Load (kg)	U_{∞} (m/s)	RPM	Angular velocity (Rad)	TSR (λ)	Torque (N.m)	Power (W)
1	0	0.32	3.71	0.39	0.57	0	0
2	1.15	0.32	3.41	0.36	0.53	0.89	0.32
3	2.15	0.32	3.28	0.34	0.51	1.61	0.55
4	3.15	0.32	3.03	0.32	0.47	2.23	0.71
5	4.15	0.32	2.74	0.29	0.43	2.86	0.82
6	5.15	0.32	2.49	0.26	0.39	3.45	0.9
7	6.15	0.32	2.43	0.25	0.38	3.98	1.01
8	7.15	0.32	2.42	0.25	0.38	5.01	1.27
9	8.15	0.32	2.22	0.23	0.35	4.94	1.15
10	9.15	0.32	1.87	0.2	0.29	8.97	1.75
11	10.15	0.32	0	0	0	10.11	0

Table 4: Test results of the performance of the LS-VACT with arm length =0.34 m

No	Load (kg)	U_{∞} (m/s)	RPM	Angular velocity (Rad/s)	TBR (λ)	Torque (N.m)	Power (W)
1	0	0.32	2.57	0.27	0.45	0	0
2	1.15	0.32	2.44	0.26	0.44	0.74	0.19
3	2.15	0.32	2.33	0.24	0.41	1.38	0.34
4	3.15	0.32	2.09	0.22	0.37	1.85	0.41
5	4.15	0.32	1.91	0.20	0.34	2.36	0.47
6	5.15	0.32	1.77	0.19	0.32	3.14	0.58
7	6.15	0.32	1.42	0.15	0.25	3.6	0.53
8	7.15	0.32	0	0	0	7.01	0

The mechanical power and torque decreased by about 27% and 32% respectively by changing the arm length from $r' = d$ to $r' = 1.7d$. The reason for this is that as the arm length increases (i.e., radius of turbine (R) increases), the angular velocity of the turbine decreases ($\omega = V/R$). This results in large wake rotational energy, and, hence, lower mechanical power output. The decrease of the turbine rotation speed (i.e., the angular velocity) combined with the increase of the wake decrease the force exerted by the water current on the advancing bucket. This in turn reduces the net torque and power output. Moreover, in this situation, the torque fluctuates due to the wake in the upstream and downstream sections, and the low difference in the magnitude of the drag between the

advancing and returning blades causes the buckets to oscillate in certain positions. These positions are circled in red in Figures 9 and 10. In addition, Figures 9 and 10 indicate that the RPM of the turbine with lower arm length is higher than that of other arm length configurations. In the latter cases, an added mass factor is produced by the oscillation of the buckets, which contributes to lower mechanical power as well.

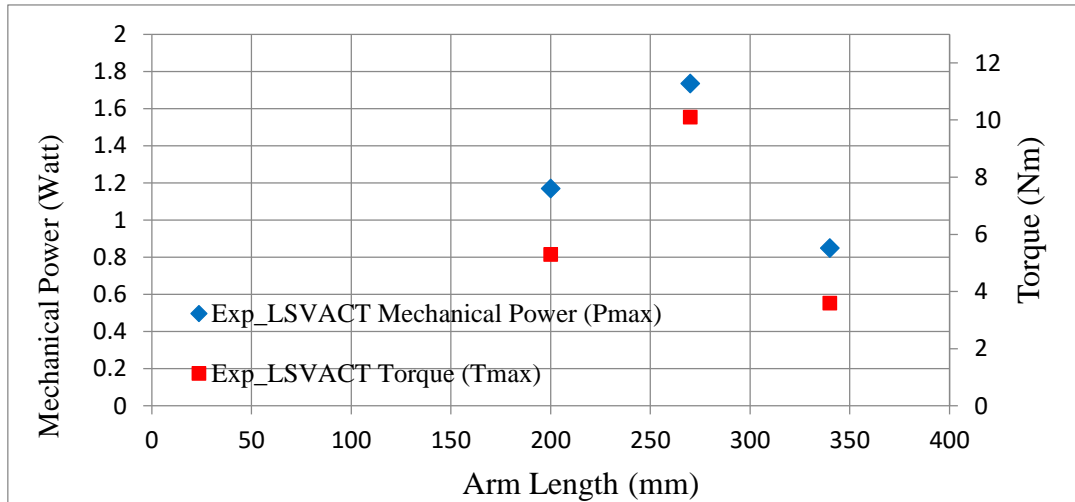


Fig. 8: The maximum power and torque of the turbine vs. different arm lengths

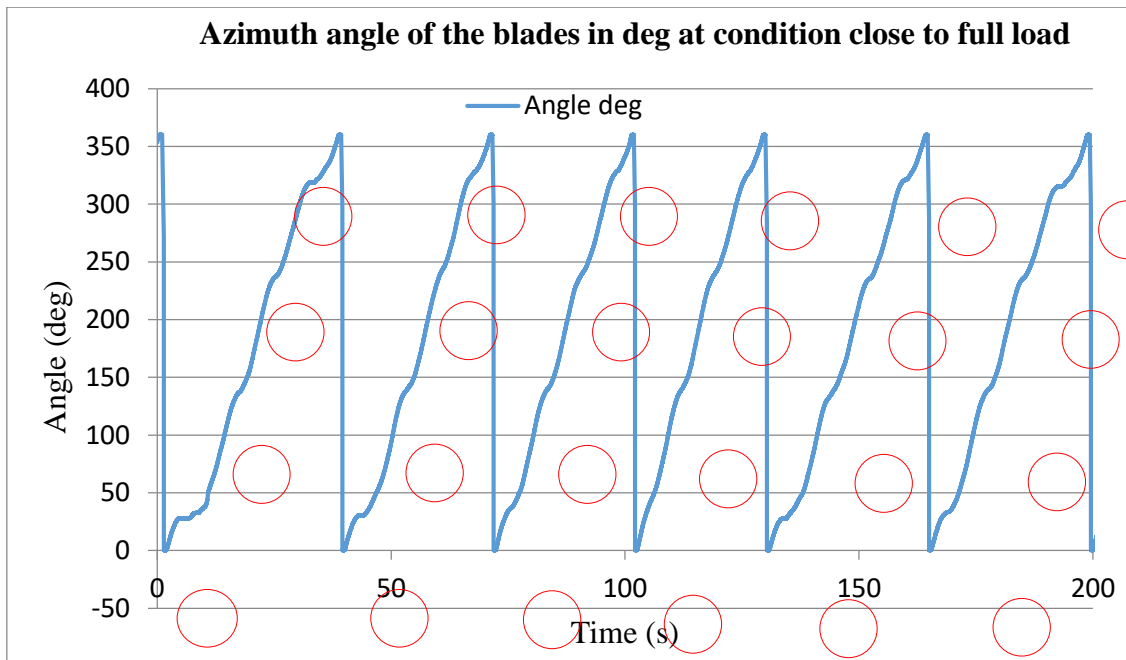


Fig. 9: Turbine bucket azimuth angle at the condition of near to the maximum loading at the current speed of 0.32 m/s and with an arm length of $r' = 1.35d$

The performance of the turbine with the optimal arm length at the remaining flow velocities of 0.17 and 0.64 m/s are illustrated in Tables 5, 6 and 7 and in Figures 11–14.

A summary of the results is shown in Figure 15.

Table 5: Test results of performance of the LS-VACT at current speed = 0.17m/s

No	Load (kg)	Current Speed (m/s)	RPM	Angular velocity (rad)	TBR (λ)	Torque (N.m)	Mechanical Power (Watt)	C_p	C_t
1	0	0.166	1.446	0.1514	0.3379	0	0	0.00	0.00
2	0.65	0.167	1.144	0.1198	0.265	0.3092	0.0371	0.03	0.09
3	1.15	0.167	1.116	0.1169	0.259	0.6247	0.0731	0.06	0.17
4	1.65	0.166	0	0	0	1.619	0	0.00	0.45

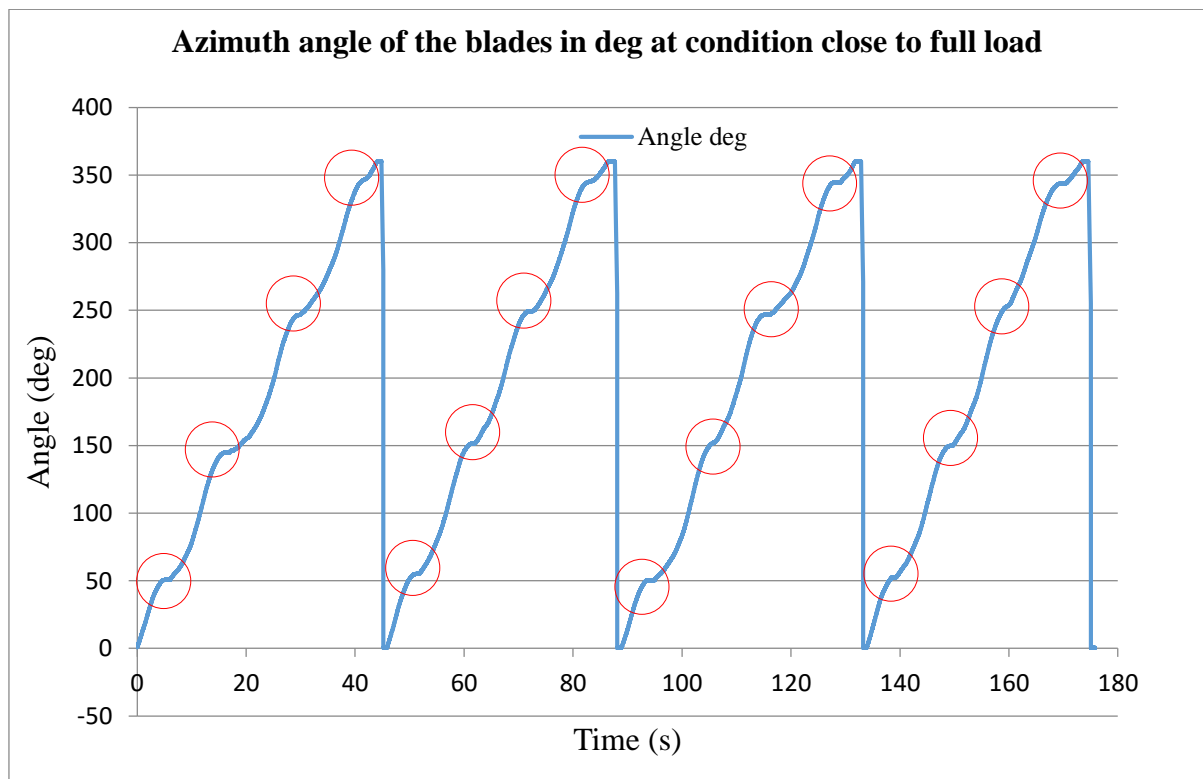


Fig. 10: Turbine blade azimuth angle at the condition of near to the maximum loading at the current speed of 0.32 m/s and with an arm length of $r' = 1.7d$

Table 6: Test results of performance of the LS-VACT at current speed = 0.32m/s

No	Load (kg)	Current Speed (m/s)	RPM	Angular velocity (rad)	TBR (λ)	Torque (N.m)	Mechanical Power (Watt)	C _p	C _t
1	0.00	0.319	3.71	0.39	0.57	0.00	0.00	0.00	0.00
2	1.15	0.318	3.41	0.36	0.53	0.89	0.32	0.04	0.07
3	2.15	0.317	3.28	0.34	0.51	1.61	0.55	0.06	0.12
4	3.15	0.317	3.03	0.32	0.47	2.23	0.71	0.08	0.17
5	4.15	0.317	2.74	0.29	0.43	2.85	0.82	0.09	0.21
6	5.15	0.317	2.49	0.26	0.39	3.45	0.90	0.10	0.26
7	6.15	0.318	2.43	0.25	0.38	3.98	1.01	0.11	0.30
8	7.15	0.317	2.42	0.25	0.38	5.01	1.27	0.14	0.38
9	8.15	0.317	2.22	0.23	0.34	4.94	1.15	0.13	0.37
10	9.15	0.317	1.87	0.20	0.29	8.97	1.75	0.19	0.52
11	10.15	0.316	0.00	0.00	0.00	10.11	0.00	0.00	0.76

Table 7: Test results of performance of the LS-VACT at current speed = 0.64m/s

No	Load (kg)	Current Speed (m/s)	RPM	Angular velocity (rad)	TBR (λ)	Torque (N.m)	Mechanical Power (Watt)	C _p	C _t
1	4.15	0.637	7.72	0.81	0.69	2.68	2.17	0.030	0.050
2	6.15	0.637	7.56	0.79	0.67	3.86	3.06	0.042	0.072
3	8.00	0.637	7.54	0.79	0.67	4.99	3.94	0.054	0.093
4	10.00	0.637	7.35	0.77	0.65	6.07	4.67	0.064	0.114
5	12.00	0.637	7.14	0.75	0.63	7.35	5.50	0.076	0.138
6	14.00	0.637	7.09	0.74	0.63	8.78	6.52	0.090	0.164
7	16.00	0.637	6.96	0.73	0.62	10.31	7.52	0.104	0.193
8	18.00	0.637	6.79	0.71	0.60	11.91	8.47	0.117	0.223
9	19.50	0.636	6.26	0.66	0.56	12.68	8.31	0.115	0.237
10	19.75	0.636	6.15	0.64	0.55	13.34	8.60	0.119	0.250
11	20.20	0.637	0.00	0.00	0.00	19.40	0.00	0.000	0.363

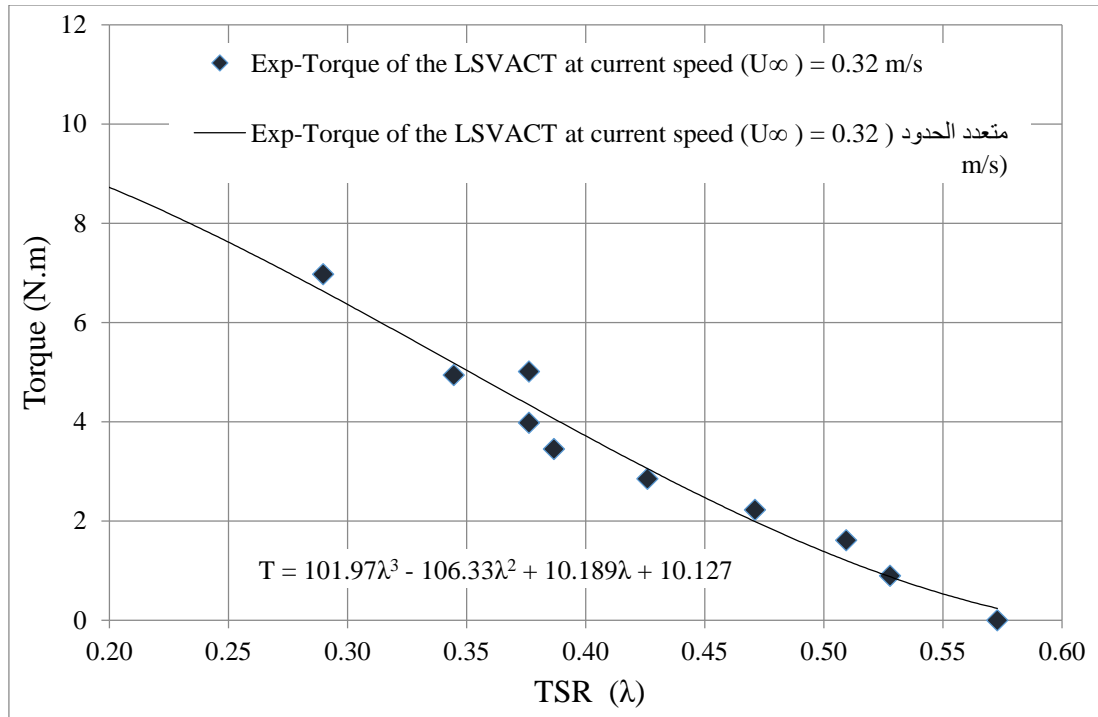


Fig. 11: Torque of the LS-VACT vs. TSR at current speed = 0.32 m/s

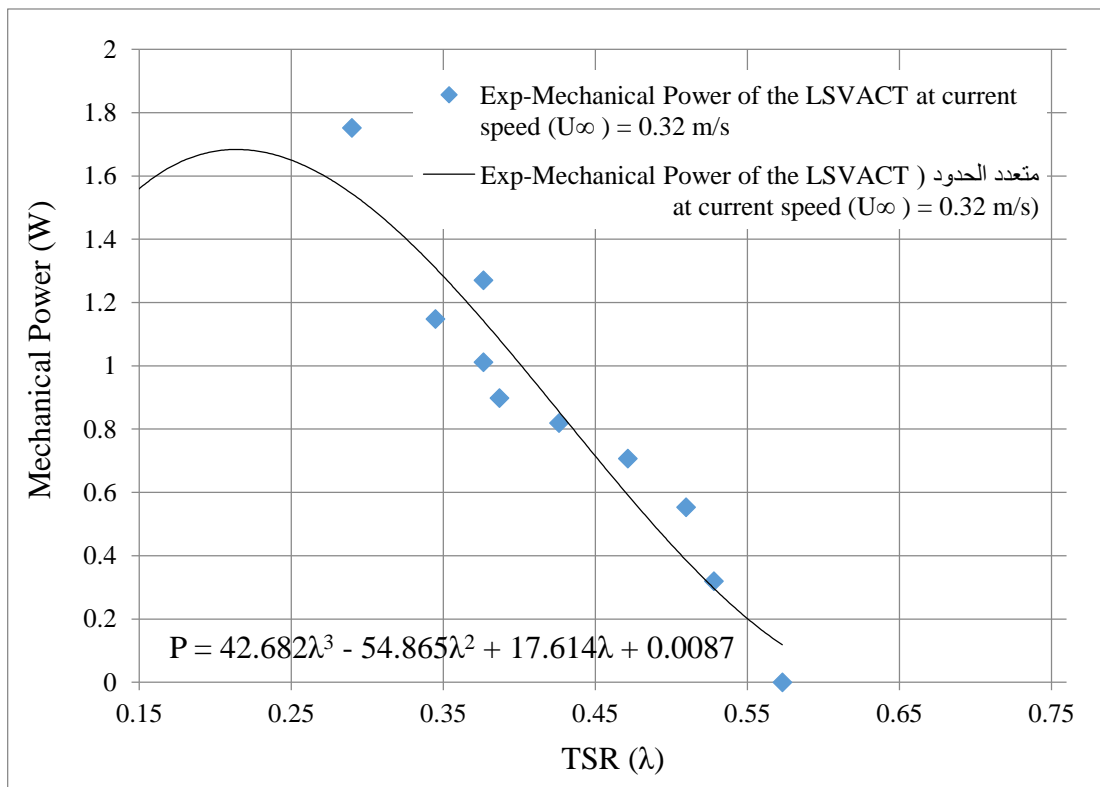


Fig. 12: Mechanical power of the LS-VACT vs. TSR at current speed = 0.32 m/s

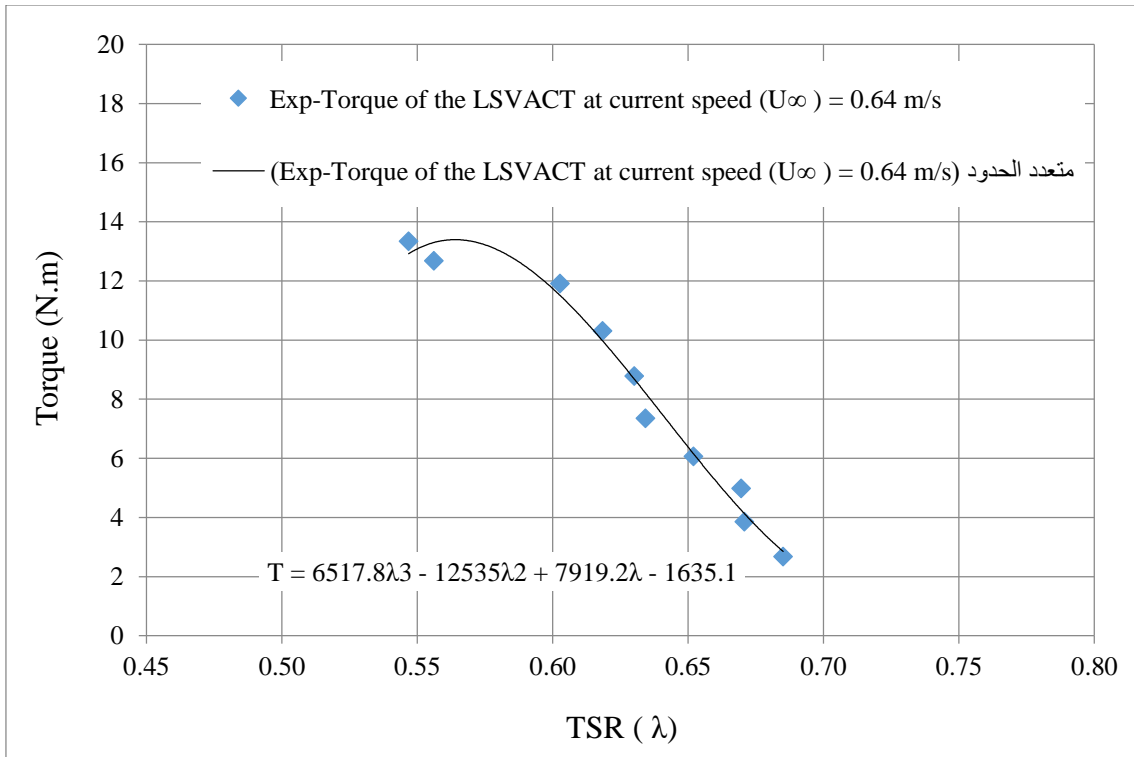


Fig. 13: Torque of the LS-VACT vs. TSR at current speed = 0.64 m/s

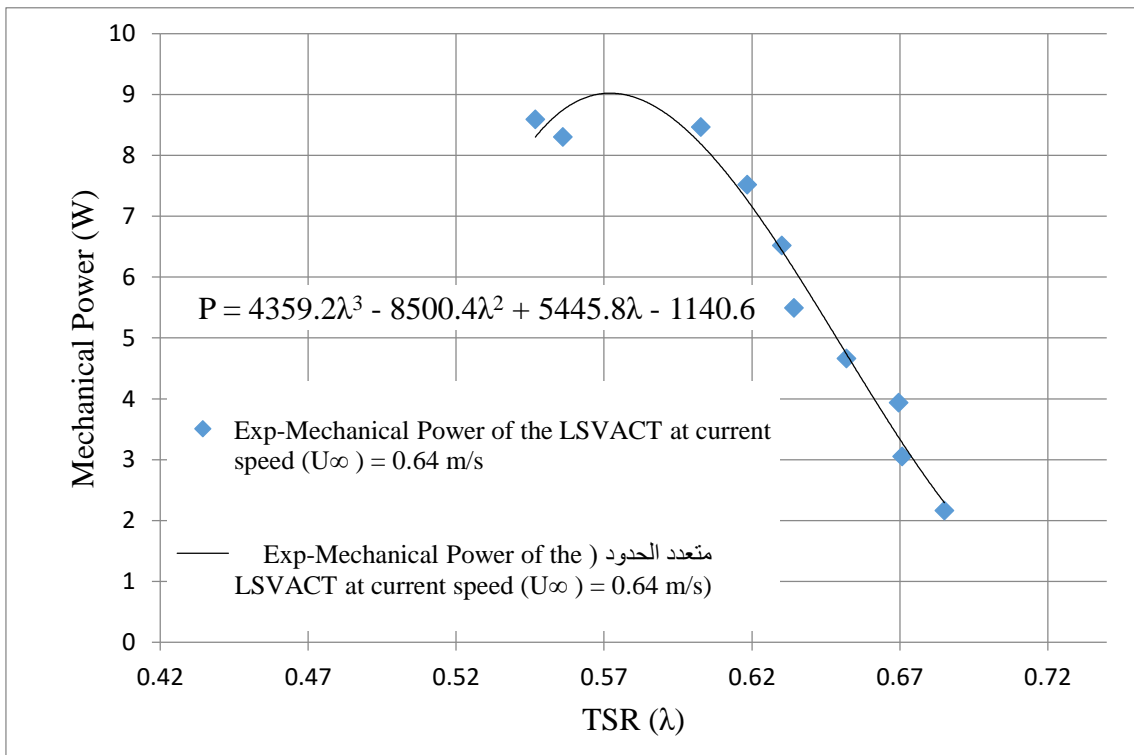


Fig. 14: Mechanical power of the LS-VACT vs. TSR at current speed = 0.64 m/s

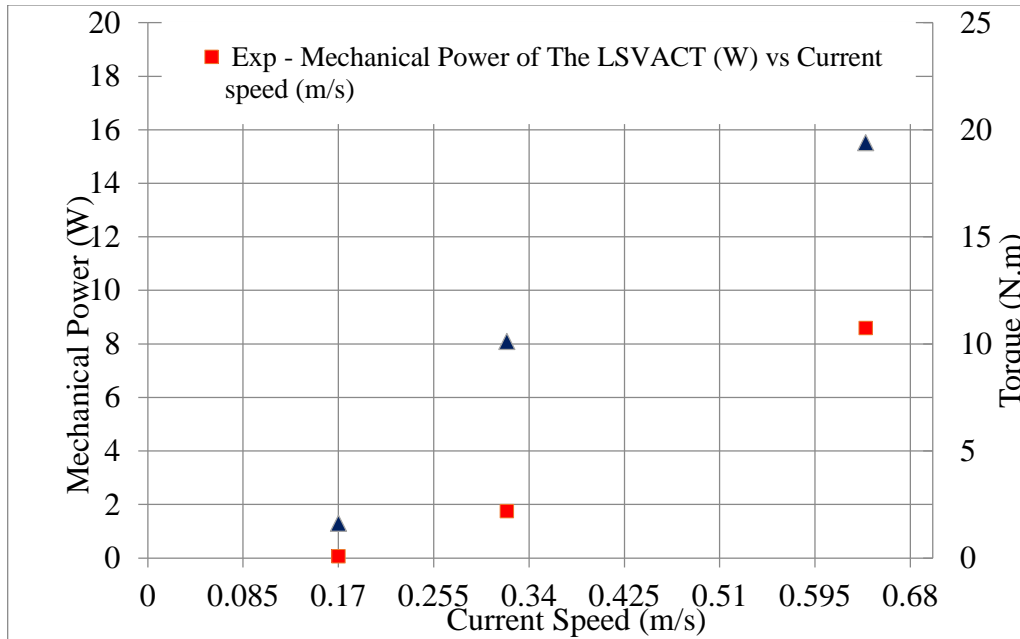


Fig. 15: Summary of the power & torque of the LS-VACT vs. current speed

The test results for this turbine revealed that the turbine has peak values for power and torque coefficients ($C_p = 0.19$ and $C_t = 0.52$) at a current speed of 0.32 m/s ($\lambda = 0.29$). However, according to the Figures 10–4, the turbine has higher power and torque outputs ($P = 8.6 \text{ watts}$ and $T = 19.4 \text{ N}\cdot\text{m}$) at a flow velocity of 0.64 m/s . These results indicate that the performance of the LS-VACT turbine at 0.17 m/s (a very low speed) is less efficient than that of the Savonius rotor in reference work [14]. However, the LS-VACT turbine produced torque values three times greater than the Savonius. The LS-VACT's performance at other velocities (0.32 and 0.64 m/s) is also acceptable due to the turbine's higher torque and its reasonable efficiency. This indicates that the turbine can integrate effectively with direct drive generators.

The oblique test conducted for the turbine bucket found the thrust and drag forces acting on the convex and concave sides of the blade at 30° intervals of the azimuth angle for several current speeds. These are shown in Figures 16 and 17. The drag coefficients obtained by conducting the experiment for both convex and concave sides of a turbine bucket at different flow velocities are shown in Figures 18 and 19.

The magnitude of the thrust, drag forces, and drag coefficients increase with increasing current speed. As a result, the results find the maximum drag coefficient at a current speed of 0.64 m/s . Peak values of the drag coefficients at this current speed are

$C_d = 1.73$ and $C_d = 0.98$ for the concave and convex sides, respectively. Moreover, the thrust forces produced by the current flow for the concave side of the blade increase as the speed increases and contribute to higher torque production. The lift forces produced by the current flow are usually small enough for the concave side to be considered negligible, but in some angular bucket positions, they can still affect the buckets at higher speeds. The lift forces for the convex side of the bucket increase as the current flow increases as well

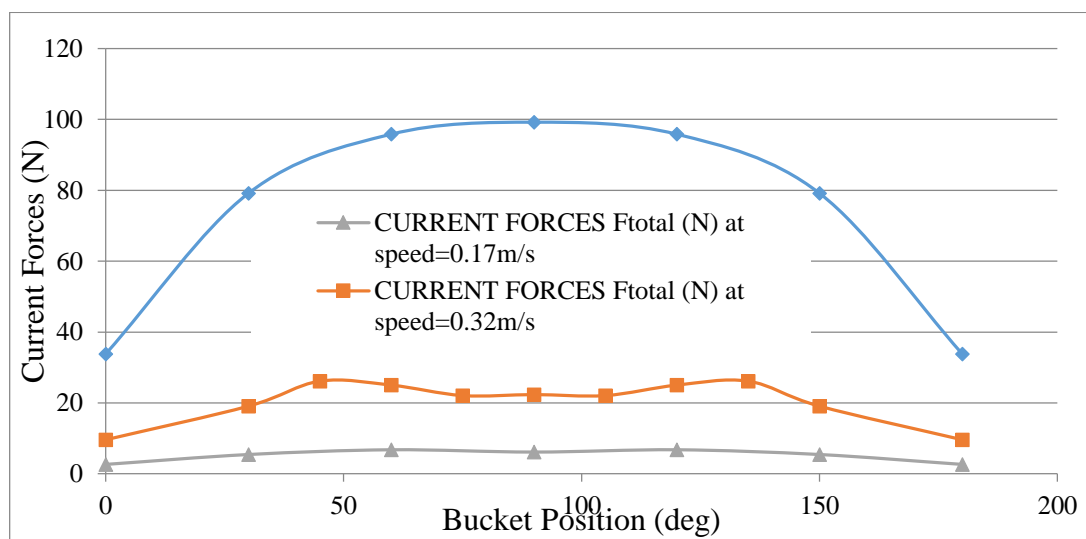


Fig. 16: Thrust forces of a single bucket of the turbine (concave side) as a function of the blade azimuth angle for azimuth angle interval $0^\circ \div 180^\circ$

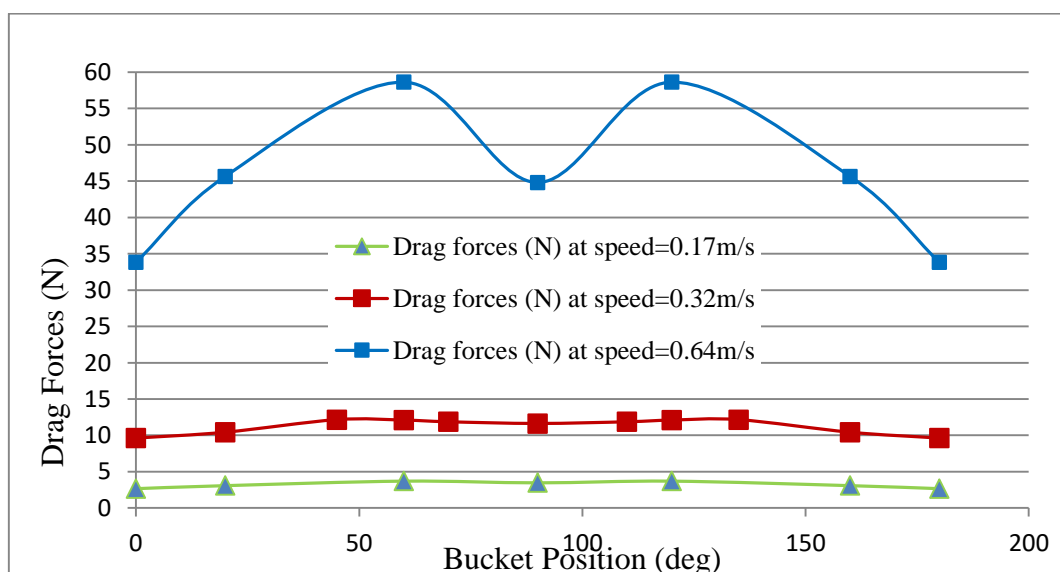


Fig. 17: Drag forces of the bucket (convex side) at several current speeds for azimuth angle interval $0^\circ \div 180^\circ$

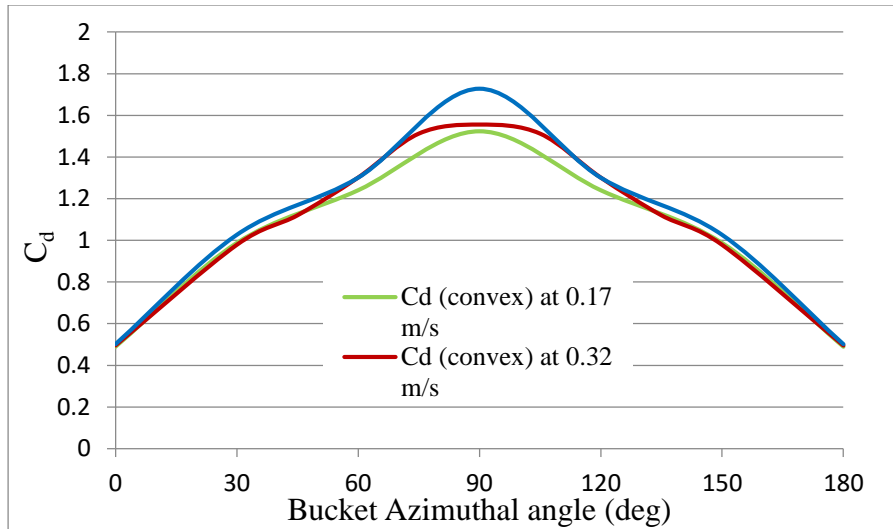


Fig. 18: Drag coefficient of a single bucket of the turbine at the concave side

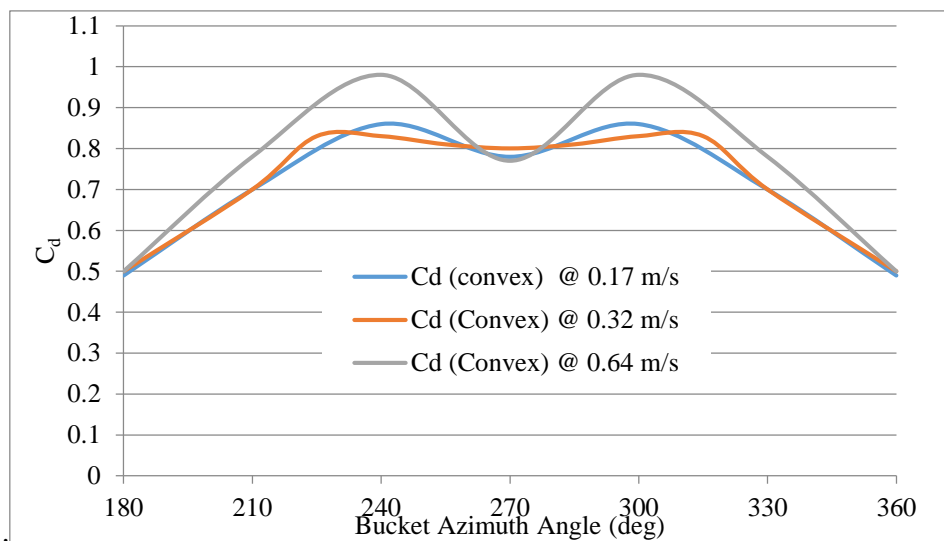


Fig. 19: Drag coefficient of a single bucket of the turbine at the convex side

5. Conclusion

This study determined the influence of arm length on the performance of low-speed vertical-axis current turbines. An experiment and a simulation were performed to investigate the effects of the arm on the performance of the turbine. Arm length values of 0.2, 0.27, and 0.34 metres were considered. The investigations showed that peak power was achieved with an arm length equal to 0.27 metres. The turbine arm ($r'=0.27$) had peak values of $C_p=0.19$ and $C_t=0.52$ at a current speed of 0.32 m/s (corresponding to $\lambda=0.29$).

However, the turbine had higher power and torque outputs ($P = 8.6$ Watts and $T = 19.4$ N·m) at a flow velocity of 0.64 m/s, even though the C_p was low. The effects of arm length on the power take-off of the turbine-generator system were also presented. The study's results may facilitate improvements in the performance of the full-scale LS-VACT as an electric turbine system. Future work could address the influence of added mass and damping on the performance of the LS-VACT, as well as the potential of increasing the accuracy of simulation results by conducting full-scale system tests using field experiments.

Acknowledgement

The authors would like to thank the Ministry of Science, Technology & Innovation (MOSTI) and Universiti Teknologi Malaysia (UTM) for financial support under project [Grant No: 03-01-06-SF1462]. Also, the authors are grateful for the support rendered to the research work by the Marine Technology Centre (MTC)/School of Mechanical Engineer at UTM.

References

1. Bedard, R., et al., An Overview of Ocean Renewable Energy Technologies. *Oceanography*, 2010. 23(2): p. 22-31.
2. Ng, K.W., W.H. Lam, and K.C. Ng, 2002-2012: 10 Years of Research Progress in Horizontal-Axis Marine Current Turbines. *Energies*, 2013. 6(3): p. 1497-1526.
3. Khan, M.J., et al., Hydrokinetic energy conversion systems and assessment of horizontal and vertical axis turbines for river and tidal applications: A technology status review. *Applied Energy*, 2009. 86(10): p. 1823-1835.
4. Ju Hyun Lee, D.H.K., Shin Hyung Rhee, In Rok Do, Byung Chul Shin, and Moon Chan Kim, Computational and Experimental Analysis for Horizontal Axis Marine Current Turbine Design, in *Second International Symposium on Marine Propulsors*. 2011: Hamburg, Germany.
5. Liu, H.W., et al., A review on the development of tidal current energy in China. *Renewable & Sustainable Energy Reviews*, 2011. 15(2): p. 1141-1146.
6. Macleod, A., et al., Wake Effects in Tidal Current Turbine Farms, in *MAREC 2002*. 2002.

7. Economic Transformation Programme: A Special Report, in Performance Management and Delivery Unit (PEMANDU), Prime Minister's Department. 2010: PUTRAJAYA, MALAYSIA. p. 1-24.
8. Government Transformation Programme The Roadmap - Executive Summary, P.M.s.D. Performance Management and Delivery Unit (PEMANDU), Editor. 2010: PUTRAJAYA, MALAYSIA. p. 1-39.
9. Yaakob, O., Abdul Ghani, M.P., Tawi, K.B., Suprayogi, D.T., Aziz, A. and Bin Jaafar, Kh.E.,. Development of Ocean Wave and Current Energy Devices. in Proceedings Seventh UMT International Symposium on Sustainability Science and Management (UMTAS). 2008. Kuala Terengganu, Malaysia.
10. Adi Maimun, F.B., Mehdi Nakisaa, Mohamad Hanafia, and Jaswara, An Innovative Vertical Axis Current Turbine Design for Low Current Speed. Jurnal Teknologi (Sciences & Engineering) 2014. 66(2): p. 177-182.
11. Aljen, A.S.M.S. and A. Maimun, Low Speed Vertical Axis Current Turbine for Electrification of Remote Areas in Malaysia, in Proceedings of the 9th International Conference on Renewable Energy Sources (RES '15). 2015, WSEAS Press: Kuala Lumpur, Malaysia. p. 75 -82.
12. Yaakob, O., K. Tawi, and D. Suprayogi. Development of vertical axis marine current turbine rotor. in RINA, Royal Institution of Naval Architects International Conference - Marine Renewable Energy - Papers. 2008.
13. Hassan, H.F., A. El-Shafie, and O.A. Karim, Tidal current turbines glance at the past and look into future prospects in Malaysia. Renewable & Sustainable Energy Reviews, 2012. 16(8): p. 5707-5717.
14. Yaakob, O.B., Experimental Studies on Savonius-type Vertical Axis Turbine for Low Marine Current Velocity. International Journal of Engineering, 2013. 26(1 (A)): p. 91-98.
15. Khan, M.J., M.T. Iqbal, and J.E. Quaicoe, River current energy conversion systems: Progress, prospects and challenges. Renewable and Sustainable Energy Reviews, 2008. 12(8): p. 2177-2193.
16. Leijon, M., et al., A low-speed generator for energy conversion from marine currents – experimental validation of simulations. Proceedings of the Institution

- of Mechanical Engineers, Part A: Journal of Power and Energy, 2008. 222(4): p. 381-388.
17. Nilsson K, S.E., Leijon M., Simulation of direct drive generators designed for underwater vertical axisturbines, in In: Proceedings of the fifth European Wave Energy Conference. 2003: Cork, Ireland. p. 1-7.
 18. Li, Y. and S.M. Calisal, Three-dimensional effects and arm effects on modeling a vertical axis tidal current turbine. Renewable Energy, 2010. 35(10): p. 2325-2334.
 19. A. A. Kadam, S.S.P., A Review Study on Savonius Wind Rotors for Accessing the. IOSR Journal of Mechanical and Civil Engineering (IOSR-JMCE), 2013. 5: p. 18-24.
 20. Kamoji, M.A., S.B. Kedare, and S.V. Prabhu, Experimental investigations on single stage modified Savonius rotor. Applied Energy, 2009. 86(7-8): p. 1064-1073.
 21. Sahim, K., et al., Experimental Study of Darrieus-Savonius Water Turbine with Deflector: Effect of Deflector on the Performance. International Journal of Rotating Machinery, 2014. 2014: p. 6.
 22. Sumpun Chaitep, T.C., Pipatpong Watanawanyoo, Hiroyuki Hirahara, Performance Evaluation of Curved Blades_VAWT. European Journal of Scientific Research, 2011. 57(3): p. 435-446.
 23. Gucl, M. U.; Sakalli, A. Analyzing the Mediterranean Sea's Dynamic Current System and Modeling of Renewable Current Energy Potential. *Journal of Marine Science and Engineering* 2024, 12(4), 671.
<https://doi.org/10.3390/jmse12040671>